solitaire-Porphyrazines: Synthetic, Structural, and Spectroscopic Investigation of Complexes of the Novel Binucleating Norphthalocyanine-2,3-dithiolato Ligand

Theodore F. Baumann,[†] Mohammad S. Nasir,[†] John W. Sibert,[†] Andrew J. P. White,[§] Marilyn M. Olmstead,[‡] David J. Williams,[§] Anthony G. M. Barrett,*[,§] and Brian M. Hoffman*[,†]

Contribution from the Departments of Chemistry, Northwestern University, Evanston, Illinois 60208, Imperial College of Science, Technology and Medicine, South Kensington, London SW7 2AY, U.K., and University of California-Davis, Davis, California 95616

Received June 7, 1996[⊗]

Abstract: We have developed the synthesis of unsymmetrical metalloporphyrazines of the form M[pz(A:B_3)], where A and B refer to two different types of peripheral functionality, and have used it to prepare new bi- and trimetallic *solitaire*-porphyrazines in which A represents a mono- or bimetallic moiety. The macrocyclic complexes described are based on the binucleating ligand, [M(norphthalocyanine-2,3-dithiolate)]$^{2-}$, [M(norpc)]$^{2-}$. This can be thought of as a metalloporphyrazine where B is a fused benzo ring; A represents two thiolates fused at the β-pyrrole positions to form a dithiolene moiety that can bind a transition-metal ion in addition to one within the macrocyclic cavity. *solitaire*-Porphyrazines have been synthesized by chelation of [(L-L)M′]$^{2+}$ to the [M(norpc)]$^{2-}$ ligand where M = "2H", Ni, Cu, or Mn-Cl, L-L is a bis(diphosphino) or bis(diamino) group and M′ = Ni, Pd, or Pt. Crystal structures have been obtained for **11b**, where the [H_2(norpc)]$^{2-}$ ligand coordinates the diphosphinopalladium moiety, [Pd(dppf)]$^{2+}$, by the two thiolate sulfur atoms at its periphery, and for **11h**, with the diaminoplatinum moiety, [Pt(teeda)]$^{2+}$, bound to the periphery of the [Ni(norpc)]$^{2-}$ ligand. In crystals of **11b** and **11h**, the molecules appear as face-to-face dimers. However, the dimer of **11b** and the two crystallographically independent dimers of **11h** each shows a distinctly different degree of overlap. The electronic absorption spectra of a series of porphyrazines in which the two peripheral sulfur atoms form thioether moieties with a modified benzyl-protecting group (**6**−**10**) show that the peripheral asymmetry of the macrocyclic framework causes a strong splitting of the ($\pi-\pi^*$) Q-band. In contrast, when the peripheral sulfurs bind a metal ion to form *solitaire*-porphyrazines **11a**−**h**, the optical spectra closely resemble that of the symmetrical pc, with unsplit Q band. The EPR spectrum of *solitaire* **11d**, where M = Cu, L-L = a bis(diphosphino) cap, M′ = Pd, has features consistent with other square-planar copper(II) porphyrins and phthalocyanines. Cyclic voltammograms of compound **11b** shows two reversible ring reductions at potentials similar to those of H_2(pc) as well as a reversible oxidation associated with the ferrocene portion of the Pd(dppf) moiety.

Introduction

Coordination compounds prepared from ligand systems capable of binding multiple metal ions are of importance in studies of electron transfer,[1] magnetic interactions,[2] optical phenomena,[3] excited-state reactivity,[4] biomimetic chemistry,[5] mixed valency,[6] and ionophoric activity.[7] One strategy for the design of multimetallic systems has involved the use of polynucleating macrocyclic ligands,[8] and, in particular, much work has been devoted to the synthesis of porphyrins[9] and phthalocyanines[10] that have been functionalized with appendages that can coordinate metal ions as well.

[†] Northwestern University.
[§] Imperial College of Science, Technology, and Medicine.
[‡] University of California-Davis.
[⊗] Abstract published in *Advance ACS Abstracts,* October 1, 1996.

(1) (a) Che, C. M.; Butler, L. G.; Grunthaner, P. J.; Gray, H. B. *Inorg. Chem.* **1985**, *24*, 4662. (b) Heuer, W. B.; Totten, M.; Rodman, G. S.; Herbert, E. J.; Tracy, H. J.; Nagle, J. K. *J. Am. Chem. Soc.* **1984**, *106*, 1163.

(2) (a) Kahn, O. *Molecular Magnetism*; VCH Publishers, Inc.: New York, 1993. (b) Gupta, G. P.; Lang, G.; Koch, C. A.; Wang, B.; Scheidt, W. R.; Reed, C. A. *Inorg. Chem.* **1990**, *29*, 4234.

(3) (a) Barigelletti, F.; De Cola, L.; Balzani, V.; Hage, R.; Haasnoot, J. G.; Reedijk, J.; Vos, J. G. *Inorg. Chem.* **1989**, *28*, 4344−4350. (b) O'Halloran, T. V.; Roberts, M. M.; Lippard, S. J. *Inorg. Chem.* **1986**, *25*, 957.

(4) (a) Che, C. M.; Butler, L. G.; Gray, H. B. *J. Am. Chem. Soc.* **1981**, *103*, 7796. (b) Fordyce, W. A.; Brummer, J. G.; Crosby, G. A. *J. Am. Chem. Soc.* **1981**, *103*, 7061.

(5) (a) Goldberg, D. P.; Koulougliotis, D.; Brudvig, G. W.; Lippard, S. J. *J. Am. Chem. Soc.* **1995**, *117*, 3134−3144. (b) Waton, S. P.; Masschelein, A.; Liu, S.; Rebek, J., Jr.; Lippard, S. J. *J. Am. Chem. Soc.* **1994**, *116*, 5196−5205. (c) Karlin, K. D.; Nasir, M. S.; Cohen, B. I.; Cruse, R. W.; Kaderli, S.; Zuberbuhler, A. D. *J. Am. Chem. Soc.* **1994**, *116*, 1324−1336. (d) Sessler, J. L.; Sibert, J. W.; Lynch, V.; Markert, J. T.; Wooten, C. L. *Inorg. Chem.* **1993**, *32*, 621−626.

(6) (a) Sharp, P. R.; Raymond, K. N.; Smart, J. C.; McKinney, R. J. *J. Am. Chem. Soc.* **1981**, *103*, 753. (b) Morrison, W. H.; Hendrickson, D. N. *Inorg. Chem.* **1975**, *14*, 2331. (c) Cowan, D. O.; Levanda, C. *J. Am. Chem. Soc.* **1972**, *94*, 9271.

(7) Gibney, B. R.; Kessissoglou, D. P.; Kampf, J. W.; Pecoraro, V. L. *Inorg. Chem.* **1994**, *33*, 4840−4849.

(8) (a) Beer, P. D.; Drew, M. G. B.; Leeson, P. B.; Lyssenko, K.; Ogden, M. I. *J. Chem. Soc., Chem. Commun.* **1995**, 929−930. (b) Bazzicalupi, C.; Bencini, A.; Bianchi, A.; Fusi, V.; Giorgi, C.; Paoletti, P.; Stefani, A.; Valtancoli, B. *Inorg. Chem.* **1995**, *34*, 552−559. (c) Coucouvanis, D.; Jonasdottir, S. G.; Christodoulou, D.; Kim, C. G.; Kampf, J. W. *Inorg. Chem.* **1993**, *32*, 2987−2988. (d) Stumpf, H. O.; Pei, Y.; Kahn, O.; Sletten, J.; Renard, J. P. *J. Am. Chem. Soc.* **1993**, *115*, 6738−6745. (e) Rockcliffe, D. A.; Martell, A. E. *Inorg. Chem.* **1993**, *32*, 3143−3152.

(9) (a) Sessler, J. L.; Weghorn, S. J.; Hiseada, Y.; Lynch, V. *Chem. Eur. J.* **1995**, *1*, 56−67. (b) Hamilton, A.; Lehn, J.-M.; Sessler, J. L. *J. Am. Chem. Soc.* **1986**, *108*, 5158−5167. (c) Basu, P.; Raitsimring, A. M.; LaBarre, M. J.; Dhawan, I. K.; Weibrecht, J. L.; Enemark, J. H. *J. Am. Chem. Soc.* **1994**, *116*, 7166−7176. (d) Drain, C. M.; Lehn, J.-M. *J. Chem. Soc. Chem. Commun.* **1994**, 2313−2315. (e) Chang, C. K. *J. Am. Chem. Soc.* **1977**, *99*, 2819−2822.

S0002-7863(96)01911-7 CCC: $12.00

We have been developing the synthesis of peripherally functionalized porphyrazines (tetraazaporphyrins), in part to prepare new polynucleating ligands based on this planar ring system.[11] The first of the series was porphyrazineoctathiolate **1**, $(pzot)^{8-}$. As a porphyrazine ring substituted with eight thiolate sulfur atoms at the β-pyrrole positions, it can coordinate four metal ions at the periphery in addition to one within the macrocyclic cavity. This ligand was designed so that the metal ions would exhibit bidentate (S−S) coordination as in dithiolene complexes, leading to pentanuclear porphyrazines that exhibit a high degree of electronic interaction between the peripheral and central metal ions as mediated by the conjugated porphyrazine core. Interestingly, a second distinct coordination mode was discovered in which two thiolate sulfur atoms from adjacent pyrroles and one meso-nitrogen atom act as ligands from the macrocycle. This tridentate (S−N−S) coordination of four dialkyltin moieties to $Ni(pzot)^{8-}$, **2**, was the first example of meso-coordination in a porphyrazine system.[11] Utilization of the bidentate (S−S) coordination sites of the octathiolate ligand was achieved through the choice of a peripherally "capping" metal ion complex that provided only two coordination sites in the *cis* configuration. A series of symmetrical pentametallic porphyrazine complexes[12] were synthesized through the reaction of $M(pzot)^{8-}$ and Ni(II)(P-P)X_2, **3**, where P−P is a chelating *cis*-diphosphine, in which the four peripheral "dithiolene" ligands are coordinated to the (P-P)Ni(II) moieties in the bidentate mode.

In this and the following paper (*J. Am. Chem. Soc.* **1996**, *118*, 10487),[13] we describe the synthesis of unsymmetrical porphyrazines of the type, $M[pz(A_n{:}B_{4-n})]$, where A and B refer to two different types of peripheral functionality and $n = 1-3$, with a focus on the molecules in which A involves a metal-chelating moiety, while B does not. This report presents the preparation and characterization of $n = 1$ macrocycles endowed with a single peripheral metal-chelation site and their use in preparing dinuclear, *solitaire*-porphyrazines[14] such as those illustrated in Chart 1. It includes the X-ray structures of a *solitaire*-porphyrazines prepared with a $[(diphophino)Pd]^{2+}$ capping moiety, **11b**, and one with a $[(diamine)Pt]^{2+}$ cap, **11h**. The spectroscopic and electrochemical properties of these complexes are compared to those of related porphyrazine and phthalocyanine complexes. The following paper (*J. Am. Chem. Soc.* **1996**, *118*, 10487)[13] describes the synthesis of $n = 2$ and 3 macrocycles and their use in preparing $n = 2$ trinuclear metal complexes, the *gemini*-porphyrazines.

Chart 1

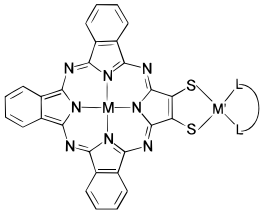

complex	M	M'	L-L [a]
11a	Ni(II)	Ni(II)	dppe
11b	"2H"	Pd(II)	dppf
11c	Ni(II)	Pd(II)	dppf
11d	Cu(II)	Pd(II)	dppf
11e	"2H"	Pt(II)	$[P(Et)_3]_2$
11f	Ni(II)	Pt(II)	$[P(Et)_3]_2$
11g	Mn(III)	Pt(II)	$[P(Et)_3]_2$
11h	Ni(II)	Pt(II)	teeda

[a]Ligand abbreviations:
dppe = (1,1'-diphenylphosphino)ethane,
dppf = (1, 1'-diphenylphosphino)ferrocene,
teeda = N,N,N',N'-(tetraethyl)ethylenediamine.

Materials and Methods

Procedures. All starting materials were purchased from Aldrich Chemical and used as received with the exceptions of (teeda)PtI_2[15] and $Na_2(mnt)$[16] which were prepared by the literature methods. THF and CH_2Cl_2 were distilled from sodium/benzophenone ketyl and CaH_2, respectively; all other solvents were used as purchased without additional purification. ^1H and ^{13}C NMR spectra were obtained using a Gemini 300 spectrometer. Electronic absorption spectra were recorded using a Hewlett-Packard HP8452A diode-array spectrophotometer. Cyclic voltammetry was done on a Cypress Systems 2000 electroanalytical system. Elemental analyses were performed by Searle Laboratories, Skokie, IL and Onieda Research Services, Whitesboro, NY and are included in supporting information (Table S11). Fast atom bombardment mass spectra (FAB-MS) were recorded locally by Dr. Doris Hung using a VG-70-250SE instrument. Electron paramagnetic resonance (EPR) spectra were measured using a modified Varian E-4 X-band spectrometer, and the field was calibrated using diphenylpicrylhydrazyl (dpph) as a standard. Powder EPR samples of Cu(norpc) (**9**) and *solitaire*-porphyrazine, [(dppf)Pd][Cu(norpc)] (**11d**), were prepared by recrystallizing about 1% of each in their corresponding diamagnetic metal-free hosts from $CHCl_3$/MeOH.

***n*-Butyl(4-chloromethyl)benzoate (4).** $SOCl_2$(12 mL, 0.165 mol) was added dropwise to a solution of 4-chloromethylbenzoic acid (25 g, 0.15 m) in DMF (25 mL). After addition was complete, the solution was heated to 85 °C for 3 h. The DMF and excess $SOCl_2$ were removed under vacuum, and the acyl chloride was quenched with *n*-BuOH (11.1 g, 0.15 M) in dry CH_2Cl_2. Removal of the solvent yielded the product as a clear oil (25.4 g, 75%); ^1H NMR ($CDCl_3$) δ (ppm) 8.0 (d, 2H), 7.40 (d, 2H), 4.55 (s, 2H), 4.15 (t, 2H), 1.75 (qn, 2H), 1.45 (sx, 2H), 0.95 (t, 3H); EI-MS 227.

Bis(4-(butyloxycarbonyl)benzyl)dithiomaleonitrile (5). A solution of **4** (9.0 g, 0.04 M), $Na_2(mnt)$ (3.72 g, 0.02 mol), and NaI in acetone was heated to reflux for 24 h. The solution was filtered hot, and the acetone was removed by rotary evaporation. The residue was taken up in $CHCl_2$ and washed three times with water. The organic layer was dried with Na_2SO_4, and the solvent was removed by rotary evaporation to yield a red oil. The product was obtained as a white solid after recrystallization from EtOH (14.6 g, 75%): mp 215−217 °C; ^1H NMR ($CDCl_3$) δ (ppm) 8.0 (d, 2H), 7.40 (d, 2H), 4.32 (s, 2H), 4.32 (t, 2H), 1.75 (qn, 2H), 1.45 (sx, 2H), 0.95 (t, 3H); ^{13}C NMR ($CDCl_3$) δ (ppm) 165.93, 139.24, 130.53, 130.26, 129.04, 121.54, 65.01, 38.75, 30.65, 19.20, 13.72; FAB-MS 523 ($M + H^+$).

(10) (a) van Nostrum, C. F.; Picken, S. J.; Nolte, R. J. M. *Angew. Chem. Int. Ed. Engl.* **1994**, *33*, 2173−2175. (b) Gürek, A. G.; Ahsen, V.; Gül, A.; Bekâroğlu, Ö. *J. Chem. Soc. Dalton Trans.* **1991**, 3367. (c) Kobayashi, N.; Higashi, Y.; Osa, T. *J. Chem. Soc., Chem. Commun.* **1994**, 1785−1786. (d) Sarigül, S.; Bekâroğlu, Ö. *Chem. Ber.* **1989**, *122*, 291−292. (e) Gürek, A. G.; Bekâroğlu, Ö. *J. Chem. Soc., Dalton Trans.* **1994**, *9*, 1419−1423. (f) Kocak, M.; Okur, A. I.; Bekâroğlu, O. *J. Chem. Soc., Dalton Trans.* **1994**, 323−326. (g) Kobayashi, N.; Opallo, M.; Osa, T. *Heterocycles* **1990**, *30*, 389. (h) Kobayashi, N.; Lever, A. B. P. *J. Am. Chem. Soc.* **1987**, *109*, 7433−7441.

(11) (a) Velazquez, C. S.; Broderick, W. E.; Sabat, M.; Barrett, A. G. M.; Hoffman, B. M. *J. Am. Chem. Soc.* **1990**, *112*, 7408−7410. (b) Velazquez, C. S.; Fox, G. A.; Broderick, W. E.; Andersen, K. A.; Anderson, O. P.; Barrett, A. G. M.; Hoffman, B. M. *J. Am. Chem. Soc.* **1992**, *114*, 7416−7424.

(12) Velazquez, C. S.; Baumann, T. F.; Olmstead, M. M.; Hope, H.; Barrett, A. G. M.; Hoffman, B. M. *J. Am. Chem. Soc.* **1993**, *115*, 9997−10003.

(13) See the following article: Sibert, J. W.; Baumann, T. F.; Williams, D. J.; White, A. J. P.; Barrett, A. G. M.; Hoffman, B. M. *J. Am. Chem. Soc.* **1996**, *118*, 10487.

(14) Baumann, T. F.; Sibert, J. W.; Olmstead, M. M.; Barrett, A. G. M.; Hoffman, B. M. *J. Am. Chem. Soc.* **1994**, *116*, 2639−2640.

(15) Dhara, S. C. *Indian J. Chem.* **1970**, *8*, 193−194.

(16) Davison, A.; Holm, R. H. *Inorg. Synth.* **1967**, *6*, 8−15.

[2,3-Bis((4-(butyloxycarbonyl)benzyl)thio)norphthalocyanato]-magnesium(II), Mg(norpc(SR)$_2$) (6). Magnesium metal (0.8 g, 0.033 mol) was added to *n*-BuOH (240 mL) and heated to reflux for 24 h. Once boiling, a small chip of iodine was added to initiate the formation of a magnesium butoxide suspension. A mixture of dinitrile **5** (2.61 g, 0.005 M) and 1,2-dicyanobenzene (16 g, 0.125 M) was added to the solution, and the mixture was heated for an additional 12 h, turning dark blue/green. The solvent was evaporated, and the residue was treated with $CHCl_3$. This solution was filtered to remove the insoluble Mg(pc) byproduct. The crude reaction product was then chromatographed on silica gel using, at first, $CHCl_3$ and then 2% MeOH in $CHCl_3$, and the major blue band was collected. Overall yield was 8−10% based on dinitrile **5**: UV/vis ($CHCl_3$) λ_{max} 358, 636, 652, 696 nm; FAB-MS 929 ($M + H^+$).

2,3-Bis((4-(butyloxycarbonyl)benzyl)thio)norphthalocyanine, H$_2$-(norpc(SR)$_2$) (7). Compound **6** (1.5 g, 1.6 mmol) was dissolved in excess CF_3CO_2H (20−25 mL) and stored in the dark for 12 h. The slurry was poured over ice water (300 mL) and neutralized with concentrated ammonium hydroxide. The black solid was collected by filtration and washed thoroughly with water, until neutral, and MeOH, until washings were colorless. The blue solid was dissolved in $CHCl_3$ and filtered to remove any insoluble black material. This blue solution was taken to dryness under rotary evaporation and dried under vacuum (1.4 g, 90%). ^{1}H NMR ($CDCl_3$) δ (ppm) 8.42 (d, 2H), 8.35 (d, 2H), 8.30 (d, 2H), 7.85 (d, 4H), 7.80 (d, 2H), 7.72 (m, 4H), 7.50 (d, 4H), 5.10 (s, 4H), 4.20 (t, 4H), 1.65 (qn, 4H), 1.35 (sx, 4H), 0.90 (t, 6H), −2.78 (s, 2H); UV/vis ($CHCl_3$) λ_{max} 346, 610, 708 nm; FAB-MS 907 ($M + H^+$).

[2,3-Bis((4-(butyloxycarbonyl)benzyl)thio)norphthalocyanato]-nickel(II), Ni(norpc(SR)$_2$) (8). The metal-free macrocycle **7** (1.0 g, 0.0011 mol), anhydrous $Ni(OAc)_2$ (1.95 g, 0.011 m), PhCl (30 mL), and DMF (10 mL) were heated to 120 °C under nitrogen for 5 h. The solvent was removed under vacuum and the solid was washed with 5% HCl in MeOH and then MeOH. The product was dried under vacuum (1.0 g, 95%): UV/vis ($CHCl_3$) λ_{max} 354, 638, 650, 696 nm; FAB-MS 965 ($M + H^+$).

[2,3-Bis((4-(butyloxycarbonyl)benzyl)thio)norphthalocyanato]-copper(II), (Cu(norpc(SR)$_2$) (9). The metal-free macrocycle **7** (1.0 g, 0.0011 mol), anhydrous $Cu(OAc)_2$ (1.95 g, 0.011 M), PhCl (30 mL), and DMF (10 mL) were heated to 120 °C under nitrogen for 5 h. The solvent was removed under vacuum, and the solid was washed with 5% HCl in MeOH and then MeOH. The product was dried under vacuum (1.0 g, 95%): UV/vis ($CHCl_3$) λ_{max} 354, 638, 650, 696 nm; FAB-MS 970 ($M + H^+$).

[2,3-Bis((4-(butyloxycarbonyl)benzyl)thio)norphthalocyanato]-manganese(III) Chloride, Mn(norpc(SR)$_2$)Cl (10). The metal-free macrocycle **7** (1.0 g, 0.0011 mol), anhydrous $MnCl_2$ (1.95 g, 0.011 M), PhCl (30 mL), and DMF (10 mL) were heated to 120 °C under nitrogen for 5 h. The solvent was removed under vacuum, and the solid was washed MeOH. The product was dried under vacuum (1.0 g, 95%): UV/vis ($CHCl_3$) λ_{max} 360, 496, 680, 749 nm; FAB-MS 961 ($M - Cl^-$).

General Procedure for Deprotection of Macrocycles 7−10. Schlenk techniques were used in this step. Macrocycle **8** (0.25 g, 0.26 mmol) was suspended in liquid NH_3 (20 mL) at −78 °C. Sodium metal (48 mg, 2.1 mmol), freshly cut under hexanes, was added in small pieces, and, once dissolved, THF (10 mL) was added to solubilize the porphyrazine. The reaction turned purple, then green, and ended as a bluish/purple color. After 30 min, NH_4Cl (70 mg, 1.3 mmol) was added to quench to excess sodium and sodium amide. The NH_3 and THF were vented off under a stream of argon yielding a fine blue powder containing sodium chloride and the disodium salt of the norphthalocyaninedithiolate. Due to the air sensitive nature of the dithiolate, no attempt at determining a yield was made, and this product was carried on to the next step.

[(1,1′-Diphenylphosphinoethane)nickel(II)][(2,3-dithiolatonorphthalocyaninato)nickel(II)] [(dppe)Ni][Ni(norpc(S$_2$)], 11a). Macrocycle **8** (0.25 g, 0.26 mmol) was deprotected by the method above. The resulting dithiolate was redissolved in deaerated MeOH (30 mL). To this solution was added $(dppe)NiCl_2$ (0.165 g, 0.31 mmol) as a solid. The blue solution was allowed to stir under argon for 2 h during which time a blue precipitate formed. This solid was filtered and washed with MeOH until washings were colorless. The solid was then dissolved in $CHCl_3$ and chromatographed on silica gel eluting with 2% MeOH/$CHCl_3$. The major blue band was collected and dried in vacuo to give 81 mg of product (30% yield): UV/vis ($CHCl_3$) λ_{max} 333, 603, 668 nm; FAB-MS 1041 ($M + H^+$).

[(1,1′-Diphenylphosphino)ferrocene]palladium(II)[2,3-dithiolatonorphthalocyanine] [(dppf)Pd][H$_2$(norpc(S$_2$))], 11b). Macrocycle **7** (0.25 g, 0.28 mmol) was deprotected, capped with $(dppf)PdCl_2$, and purified using the procedure above to yield 110 mg of product (35% yield). The product was recrystallized from CH_2Cl_2/MeOH: ^{1}H NMR ($CDCl_3$) δ (ppm) 9.59 (d, aromatic), 9.25 (d, aromatic), 9.15 (d, aromatic), 8.30 (m, aromatic), 8.05 (m, aromatic), 7.65 (t, aromatic), 7.55 (t, aromatic), 4.48 (d, 4H-Cp), −0.75 (s, 2H-internal); UV/vis ($CHCl_3$) λ_{max} 337, 592, 643, 722 nm; FAB-MS 1185 ($M + H^+$).

[(1,1′-Diphenylphosphino)ferrocene]palladium(II)[2,3-dithiolatonorphthalocyaninato)nickel(II)] [(dppf)Pd][Ni(norpc(S$_2$))], 11c). Macrocycle **8** (0.25 g, 0.26 mmol) was deprotected, capped with $(dppf)PdCl_2$, and purified using the procedure above to yield 97 mg of product (30% yield): UV/vis ($CHCl_3$) λ_{max} 333, 603, 666 nm; FAB-MS 1244 ($M + H^+$).

[(1,1′-Diphenylphosphino)ferrocene]palladium(II)[(2,3-dithiolatonorphthalocyaninato)copper(II)] [(dppf)Pd][Cu(norpc(S$_2$))], 11d). Macrocycle **9** (0.25 g, 0.26 mmol) was deprotected, capped with $(dppf)PdCl_2$, and purified using the procedure above to yield 80 mg of product (25% yield): UV/vis ($CHCl_3$) λ_{max} 339, 606, 679 nm; FAB-MS 1250 ($M + H^+$).

[(Bis-triethylphosphine)]platinum(II)[2,3-dithiolatonorphthalocyanine] [(C$_2$H$_5$)$_3$P]$_2$Pt[H$_2$(norpc(S$_2$))], 11e). Macrocycle **7** (0.25 g, 0.28 mmol) was deprotected, capped with $(Et_3P)_2PtCl_2$, and purified using the procedure above to yield 95 mg of product (35% yield): UV/vis ($CHCl_3$) λ_{max} 338, 591, 644, 725 nm; FAB-MS 959 ($M + H^+$).

[(Bis-triethylphosphine)]platinum(II)[(2,3-dithiolatonorphthalocyaninato)nickel(II)] [(C$_2$H$_5$)$_3$P]$_2$Pt[Ni(norpc(S$_2$))], 11f). Macrocycle **8** (0.25 g, 0.26 mmol) was deprotected, capped with $(Et_3P)_2PtCl_2$, and purified using the procedure above to yield 93 mg of product (35% yield): UV/vis ($CHCl_3$) λ_{max} 333, 602, 669 nm; FAB-MS 1018 ($M + H^+$).

[(Bis-triethylphosphine)]platinum(II)[(2,3-dithiolatonorphthalocyaninato)manganese(III)chloride] [(C$_2$H$_5$)$_3$P]$_2$Pt [Mn(norpc(S$_2$))-Cl], 11g). Macrocycle **10** (0.25 g, 0.25 mmol) was deprotected, capped with $(Et_3P)_2PtCl_2$, and purified using the procedure above to yield 82 mg of product (30% yield): UV/vis ($CHCl_3$) λ_{max} 352, 516, 656, 712 nm; FAB-MS 1047 ($M - Cl^-$).

***[N,N,N′,N′*-Tetraethylethylenediamine]platinum(II)[(2,3-dithiolatonorphthalocyaninato)nickel(II)] [(teeda)Pt][Ni(norpc(S$_2$))], 11h).** Macrocycle **9** (0.25 g, 0.26 mmol) was deprotected, capped with (teeda)-PtI_2, and purified using the procedure above to yield 0.065 mg of product (25% yield): UV/vis ($CHCl_3$) λ_{max} 335, 609, 669 nm; FAB-MS 950 ($M + H^+$).

X-ray Crystallography of Complex 11b. The crystal selected for data collection was mounted in the cold stream (130 K) of a Siemens P4 diffractometer equipped with a LT-2 low-temperature apparatus. The radiation employed was Ni-filtered Cu Kα from a Siemens rotating anode source operating at 15 kW. A linear decay of 4.5% in the intensities of three standard reflections was observed during data collection, and the data were scaled to adjust for this decay. Neutral atom scattering factors were from a common source. The structure was solved in the space group *C*2/*c* using direct and difference Fourier methods.[17] In addition to compound **11b**, the structure contains two molecules of solvent CH_2Cl_2. Hydrogens bonded to carbon were added geometrically and refined by use of a riding model and isotropic thermal parameters equal to 1.2 times the equivalent isotropic thermal parameter of the bonded carbon. Hydrogens bonded to the nitrogen atoms of the porphyrazine core were located on a difference Fourier map. In subsequent cycles of refinement their positional parameters were allowed to vary, but their isotropic thermal parameters were fixed at a

(17) Tables of neutral atom scattering factors, f' and f'', and absorption coefficients are from International Tables for Crystallography; Wilson, A. J. C., Ed.; Kluwer Academic Publishers: Dordrecht, 1992; Vol. C, Tables 6.1.1.3 (pp 500−502), 4.2.6.8 (pp 219−222), and 4.2.4.2 (pp 193−199), respectively.

Scheme 1[a]

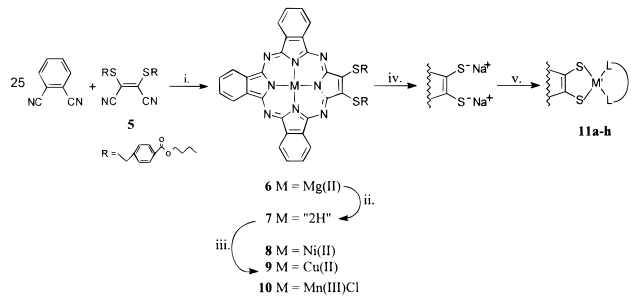

[a] (i) $Mg(OBu)_2$, BuOH, reflux, 24 h; (ii) CF_3COOH, 25 °C, 12 h; (iii) $M(II)(X)_2$ (X = $^-$OAc, Cl^-), PhCl, DMF, 100 °C, 4 h; (iv) Na (4 equiv), NH_3, THF, −33 °C, 0.5 h; (v) $L_2M'X_2$, MeOH, 25 °C, 1 h.

typical value of 0.03 Å^2. An absorption correction (XABS[18]) was applied. Final refinement was by full-matrix least-squares methods[19] based on F^2, using all data, with anisotropic thermal parameters for all non-hydrogen atoms. The largest feature on a final difference map was 0.71 eÅ^{-3} in magnitude, 2.2 Å from the chlorine of a CH_2Cl_2.

X-ray Crystallography of Complex 11h. Data for a thin green/black plate were measured at room temperature on a Siemens P4 rotating anode diffractometer with graphite monochromated Cu-K_α radiation using ω-scans. Independent reflections (7827) were measured ($2\theta \leq 100°$), and of these 6497 had $|F_o| > 4\sigma(|F_o|)$ and were considered to be observed. The data were corrected for Lorentz and polarization factors and for absorption-numerical correction for a face-indexed crystal-minimum and maximum transmission factors 0.207 and 0.848, respectively.

The structure was solved by direct methods, and all the major occupancy non-hydrogen atoms in the complexes were refined anisotropically. A ΔF map revealed the presence of 60:40 disorder in the teeda ligand of one of the two independent complexes; the minor occupancy carbon and nitrogen atoms were refined isotropically. The structure was also found to contain two crystallographically independent 50% occupancy included $CHCl_3$ molecules: only the chlorine atoms were refined anisotropically. All hydrogen atoms were placed in idealized positions, assigned isotropic thermal parameters, $U(H) = 1.2U_{eq}(C)$ [$U(H) = 1.5_{eq}(C-Me)$], and allowed to ride on their parent carbon atoms. Refinement was by full-matrix least squares based on F^2 and converged [Δ/σ ratios less than 1σ for all parameters] to give $R_1 = 0.078$, $wR_2 = 0.201$ for 1028 parameters. The maximum and minimum residual electron densities in the final ΔF map were 2.42 and −1.93 eÅ^{-3}, respectively, in the regions of the platinum atoms. The somewhat high value of R_1 is probably due to the poor crystal quality—the thin plates tended to be deformed and gave diffuse diffraction. Computations were carried out on an 50 MHz 486 PC computer using the SHELXTL-PC program system.[20]

Results and Discussion

Synthesis of Bi- and Trimetallic *solitaire* Porphyrazines. The synthesis of the *solitaire*-porphyrazines, **11a**−**h**, begins with the mixed condensation of a protected dithiomaleonitrile derivative and the commercially available 1,2-dicyanobenzene (Scheme 1). Normally a mixed cyclization would yield all six of the porphyrazines that can result from the combination of the two dinitriles in the reaction mixture. This problem is avoided by using an excess of 1,2-dicyanobenzene to ensure that only two major products are formed, Mg(pc) and $Mg(norpc(SR)_2)$. Mg(pc) is quite insoluble in most organic solvents, whereas $Mg(norpc(SR)_2)$ is soluble with the proper selection of a thiolate protecting group. The 4-(butyloxycarbonyl)benzyl (BCB) protecting group was chosen for several reasons. (i) The benzyl protecting group is well-established in thiolate chemistry as being robust yet readily cleaved with sodium metal in liquid ammonia.[21] (ii) Alkylation of $Na_2(mnt)$ with butyl(4-chloromethyl)benzoate produces dinitrile **4** in high yields which can be readily cyclized using the magnesium alkoxide method.[22,23] (iii) Most importantly, the butyl ester lends sufficient solubility for the isolation and purification of the protected porphyrazine. In addition, transesterification which occurs during the butoxide cyclization does not yield new products, as occurs with other ester-substituted benzyl derivatives. (iv) Placement of the electron-withdrawing ester moiety in the para position facilitates the reductive cleavage of the benzyl protecting group, relative to an unsubstituted benzyl group.

In practice, mixed condensation of BCB-protected dithiomaleonitrile **5** and 1,2-dicyanobenzene (25-fold excess) followed by treatment of the reaction product with $CHCl_3$ allows for the easy isolation of **6** in reasonable yield (15%). The magnesium atom is cleanly removed from **6** using neat trifluoroacetic acid to give **7**, and remetalation with nickel, copper, and manganese to give **8**−**10** proceeds smoothly using high-temperature metalation conditions.[24] Use of M = Ni(II) and Cu(II) leads to the $M(II)(norpc(SR)_2)$, **8** and **9**; Mn(II) also incorporates into the macrocyclic cavity but promptly air-oxidizes to Mn(III) within the metalation reaction presumably with an axial chloride ligand. Debenzylation of **7**−**10** was achieved by reductive cleavage with sodium metal in liquid ammonia. The resulting norphthalocyanine dithiolate is air-sensitive, and Schlenk techniques were employed during all manipulations. The dithiolate dissolves in deaerated MeOH to give a dark blue solution that may be subsequently treated with various "capping" reagents to give air-stable bi- and trimetallic *solitaire*-porphyrazine complexes in yields of 25−35% based on the starting BCB-protected porphyrazine. Chart 1 lists the *solitaire*-porphyrazines synthesized.

X-ray Crystal Structure of 11b. *solitaire*-Porphyrazine **11b** has a [palladium(bis(1,1′-diphenylphosphino)ferrocene)]$^{2+}$ moiety coordinated to the peripheral dithiolate of the $[H_2(norpc(S_2^-))]^{2-}$ core. The pertinent parameters for the data collection and structure determination of **11b** are compiled in Table 1, and its molecular structure is shown in Figure 1a. A comparison of bond lengths and bond angles for **3**,[12] **11b**, **11h**, and M(pc)[25] is presented in Table 2. The macrocyclic ring of **11b** is essentially planar with only modest deviations of the peripheral fused benzene rings out of the least-squares plane defined by the four pyrrole nitrogen atoms. The geometry of the norphthalocyanine portion is similar to that of pc, with only slight variations seen in the pyrrole containing the fused dithiolene moiety. However, the asymmetry at the periphery is nonetheless apparent at the core in that the internal N−H protons are resolved in the X-ray structure, being localized on pyrrole nitrogens N1 and N3.

The four-coordinate palladium ion is chelated by the two dithiolene sulfurs and by the two phosphorus atoms of the 1,1′-bis(diphenylphosphino)ferrocene moiety. As seen with the tetranuclear complexes of nickel porphyrazineoctathiolate,[12] $[Ni(pzot)]^{8-}$, the dithiolene unit of **11b** adjusts itself in order to chelate the palladium ion by a swing of the C_β−S bond. Whereas the C_β−C_β−S bond angle for the unconstrained reference, Mg(octakis(methylthio)porphyrazine), Mg(otmp),[11b]

(18) XABS2: an empirical absorption correction program. Parkin, S.; Moezzi, B.; Hope, H. *J. Appl. Cryst.* **1995**, *28*, 53−56.

(19) SHELXL-93 (Sheldrick, G. M. *J. Appl. Cryst.* 1994, in preparation.)

(20) SHELXTLPC version 5.03, Siemens Analytical X-Ray Instruments, Madison, WI, 1994.

(21) Greene, T. W.; P. G. M. In *Protective Groups in Organic Synthesis*; John Wiley and Sons Inc.: New York, 1991; Chapter 6, pp 277−308.

(22) Linstead, R. P.; Whalley, M. *J. Chem. Soc.* **1952**, 4839−4846.

(23) Schramm, C. J.; Hoffman, B. M. *Inorg. Chem.* **1980**, *19*, 383−385.

(24) Buchler, J. W. In *The Porphyrins*; Dolphin, D., Ed.; Academic Press: New York, 1978; Vol. 1, Chapter 10.

(25) Schramm, C. J.; Scaringe, R. P.; Stojakovic, D. R.; Hoffman, B. M.; Ibers, J. A.; Marks, T. J. *J. Am. Chem. Soc.* **1980**, *102*, 6702−6709.

Table 1. Crystal Data and Structure Refinement for *solitaire*-Porphyrazines **11b** and **11h**

	11b	**11h**
empirical formula	$C_{64}H_{46}Cl_4FeN_8P_2PdS_2$	$C_{38}H_{36}N_{10}NiPtS_2 \cdot {}^1/_2CHCl_3$
formula weight	1357.20	1010.37
temperature	125(2) K	293(2) K
wavelength	1.54178 Å	1.54178
crystal system	monoclinic	triclinic
space group	*C*2/*c*	*P*1
unit cell dimensions	$a = 37.916(7)$ Å	$a = 13.160(12)$ Å
	$b = 10.807(1)$ Å	$b = 16.526(10)$ Å
	$c = 29.588(4)$ Å	$c = 20.374(11)$ Å
	$\alpha = 90°$	$\alpha = 113.80(4)°$
	$\beta = 109.85(1)°$	$\beta = 92.93(6)°$
	$\gamma = 90°$	$\gamma = 98.34(6)°$
vol.	11404(3) Å^3	3982(5) Å^3
Z	8	4[a]
density (calc)	1.581 mg/m^3	1.685 mg/m^3
absorption coefficient	7.929 mm^{-1}	9.310 mm^{-1}
F(000)	5504	2004
crystal size	0.18 × 0.08 × 0.03 mm	0.30 × 0.20 × 0.02 mm
θ range for data collection	2.48−56.07°	2.39−50.00°
index ranges	$-40 \le h \le 38$	$0 \le h \le 11$
	$0 \le k \le 11$	$-16 \le k \le 16$
	$0 \le l \le 31$	$-20 \le l \le 20$
reflections collected	8082	7827
independent reflections	7439 ($R_{int} = 0.024$)	7827 ($R_{int} = 0.000$)
absorption correction	XABS2[b]	integration
refinement method	full-matrix least squares on F^2	
data/restraints/parameters	7439/0/749	7819/25/1028
goodness-of-fit[c] on F^2	1.022	1.088
final *R* indices[d] [$I > 2\sigma(I)$]	$R_1 = 0.0469$, $wR_2 = 0.1140$	$R_1 = 0.0775$, $wR_2 = 0.2007$
R indices (all data)	$R_1 = 0.0611$, $wR_2 = 0.1245$	$R_1 = 0.0917$, $wR_2 = 0.2149$
largest diff. peak and hole	0.708 and −0.745 e Å^{-3}	2.415 and −1.929 e Å^{-3}

[a] There are two crystallographically independent molecules in the asymmetric unit. [b] XABS2 (Parkin, S.; Moezzi, B.; Hope, H. *J. Appl. Cryst.* **1995**, *28*, 53−56) calculates 24 coefficients from a least-squares fit of ($1/A$ vs $\sin^2(\theta)$) to a cubic equation in $\sin^2\theta$ by minimization of F_o^2 and F_c^2 differences. [c] Goodness-of-fit = $[\sum[w(F_o^2 - F_c^2)^2]/(M - N)]^{1/2}$ where *M* is the number of reflections and *N* is the number of parameters refined. [d] $R_1 = \sum||F_o| - |F_c||/\sum|F_o|$; $wR_2 = [\sum[w(F_o^2 - F_c^2)^2]/\sum[w(F_o^2)^2]]^{1/2}$.

is 128.5(35)°, the same angle in **11b** closes to 124.0(7)°. Likewise, the distance between the sulfurs decreases from 3.53 Å in Mg(omtp) to 3.31 Å in **11b**.

To our knowledge, there is only one reported crystal structure of a (P−P)Pd(II) complex bearing a dithiolate chelating ligand, that of (dithiooxalato-S,S′)bis(trimethylphosphine)palladium-(II).[26] The Pd−S and Pd−P bond distances for **11b** of 2.316-(5) and 2.326(4) Å, respectively, are similar to the values for that structure (2.300 and 2.334 Å). The bond angles around palladium are not all equal for **11b**, with S−Pd−S and P−Pd−P angles of 90.6(5)° and 97.9(5)°, respectively. These values differ slightly (∼3°) from the literature reference, probably because the phosphine ligands are different. The ferrocene portion of the diphosphine cap is structurally similar to free ferrocene, and the average Fe−C bond distance of 2.043(6) Å is comparable to the reported value of 2.04(2) Å.[27]

Each macrocycle in the unit cell stacks with an centrosymmetrically-related porphyrazine to form a back-to-back "dimer" (Figure 2a). The interplanar separation of the overlapped portions of the porphyrazine planes in each pair is 3.13 Å. The degree of overlap of the two porphyrazine planes in the dimer, however, is limited due to the bulky 1,1′-(diphenylphosphino)-ferrocene moiety. The macrocycles pack is dimerized slipped-stack chains with significant $\pi-\pi$ overlap between the fused isoindole rings of adjacent sets of dimers (Figure 3a). The phenyl groups of the dppf ligand are brought into the range for numerous edge-to-face phenyl-phenyl interactions between the stacked chains of porphyrazine dimers.

X-ray Crystal Structure of 11h. *solitaire*-Porphyrazine **11h** has a platinum[*N*,*N*,*N*′,*N*′-tetraethylenediamine]$^{2+}$ moiety coordinated to the peripheral dithiolate of the [Ni(norpc(S_2^-))]$^{2-}$ core, and Table 1 contains the pertinent parameters for the data collection and structure determination of **11h**. Figure 1b illustrates one (**A**) of the two crystallographically independent molecules (**A** and **B**) of **11h** present in the asymmetric unit; the other molecule (**B**) has only slight differences in the orientations of the ethyl groups of the teeda ligand. The central nickel atoms in both **A** and **B** adopt normal square-planar geometries with Ni−N bond lengths in the range 1.88(1)−1.91-(1) Å for molecule **A** and 1.86(1)−1.88(1) Å for molecule **B**. The peripheral platinum atoms also have conventional square planar geometries with Pt−S distances of 2.273(4) and 2.265-(5) Å in **A** and 2.267(5) and 2.251(5) Å in **B**; the Pt−N distances in both **A** and **B** are all normal at *ca*. 2.06 Å. The S−Pt−S angles are 91.2(2) and 91.7(2)° in **A** and **B**, respectively, reflecting the optimization of the norphthalocyanine-2,3-dithiolato chelate by a swing of the C_β−S bond as noted above for **11b**; the N−Pt−N angles are slightly contracted at 84.7(6) and 84.1(5)° in **A** and **B**, respectively, compared to the expansion for P−Pd−P in **11b**.

The principal difference between the two molecules of **11h** is in the relative planarities of the porphyrazine units. In molecule **A** this unit exhibits a very pronounced "dishing"—the central core of nickel-coordinated nitrogen atoms is coplanar to within 0.004 Å (with the nickel atom deviating by 0.05 Å "below" this plane), whereas the platinum atom and the centroids of the three exocyclic six-membered rings [associated with N(22), N(23), and N(24)] lie 0.35, 0.31, 0.46, and 0.18 Å "above" this plane, respectively. In contrast, molecule **B** is essentially planar. The comparative values for molecule **B** (in which the four nickel-coordinated nitrogen atooms are coplanar to within 0.02 Å) are 0.007 Å below and 0.22, 0.11, 0.02, and

(26) Cowan, R. L.; Pourreau, D. B.; Rheingold, A. L.; Geib, S. J.; Trogler, W. C. *Inorg. Chem.* **1987**, *26*, 259.
(27) Dunitz, J. D.; Orgel, L. E.; Rich, A. *Acta Crystallogr.* **1956**, *9*, 373.

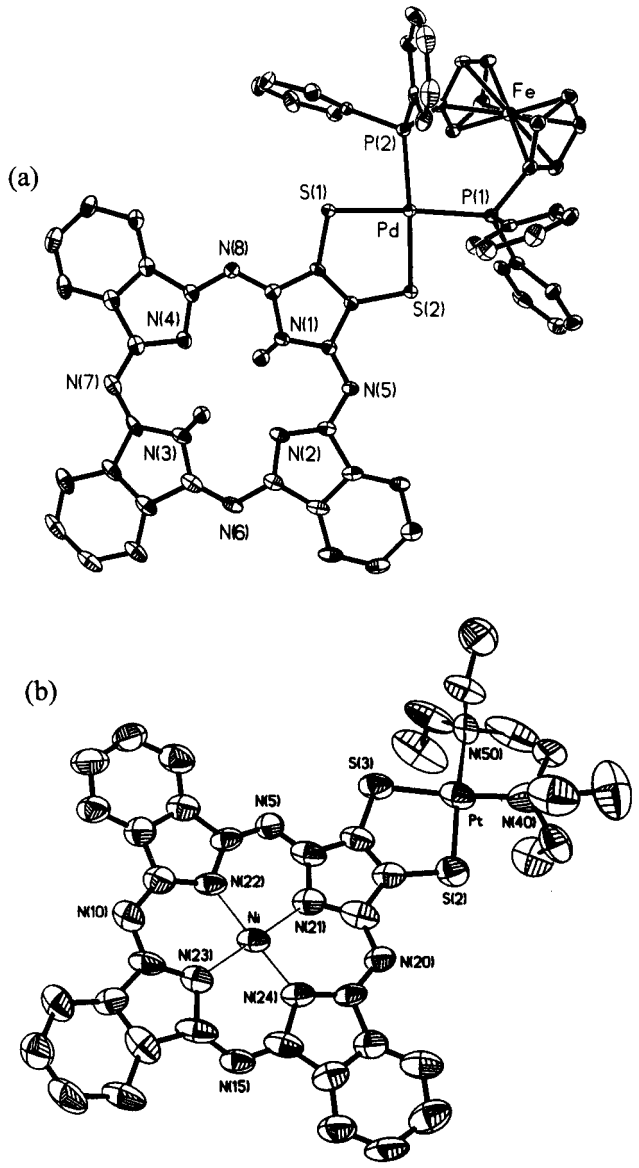

Figure 1. Structures of **11b** and **11hA** showing 50% probability thermal ellipsoids. For clarity, the heteroatoms have been labeled and the hydrogen atoms have been omitted.

0.11 Å above for the deviations of the nickel atom, platinum atom, and exocyclic ring centroids, respectively.

As with **11b**, each of the independent molecules of **11h** packs with a centrosymmetrically-related counterpart to form a back-to-back "dimer". Although the interplanar separations are very similar, the relative degrees of overlap between the porphyrazine rings in each of the three cases (**11b** and **11h A** and **B**) is markedly different, with the overlap being least for **11b** (Figure 2). For molecule **11hA**, ring−ring overlap is maximized (Figure 2b), though at the expense of the marked dishing of the molecule (Figure S1) described above. The mean interplanar separation between the planes define by the four nickel-coordinated nitrogens atoms is 3.20 Å, the Ni···Ni separation being 3.41 Å, i.e., the molecules are sheared by *ca*. 1.2 Å with respect to each other. The shortest intermolecular Ni···N contact is 3.28 Å to Ni(24), whilst the sulfur atom S(2), which overlays an exocyclic six-membered ring, is *ca*. 4.0 Å distant from the mean plane of this ring. The mean interplanar separation between the overlapping isoindole rings is *ca*. 3.6 Å. Molecules of type 11hB, which have a much more planar geometry than **11hA** (Figure S2), have an offset back-to-back "dimer" relationship similar to but less extreme than that of **11b** (Figure 2c). The

Table 2. Comparison of Symmetry-Averaged Bond Lengths and Bond Angles for Complex **11b**, **11h**, M(pc),[a] and (**3**) $[(dppe)Ni]_4[Ni(pzot)]$[b]

	11b	**11h**	M(pc)	**3**
		Bond Distance (Å)		
$Ni-N_p$		1.88(2)	1.88(6)	1.87(3)
$C_\alpha-N_p$	1.369(8)	1.38(2)	1.376	1.41(1)
$C_\alpha-C_\beta$	1.455(9)	1.45(2)	1.453	1.46(3)
$C_\beta-C_\beta$	1.392(7)	1.37(3)	1.395	1.36(1)
$C_\alpha-N_m$	1.328(8)	1.33(2)	1.328	1.34(3)
$C_\beta-C_\gamma$	1.387(9)	1.39(3)	1.387	
$C_\gamma-C_\delta$	1.382(9)	1.37(3)	1.388	
$C_\delta-C_\delta$	1.391(9)	1.38(3)	1.394	
$C_\beta-S$	1.739(8)	1.73(2)	1.71(1)	
S···S	3.31	3.30	3.25	
		Bond Angles (deg)		
N_p-Ni-N_p		89.9(6)	90	90.0(17)
N_p-Ni-N_p'		177.1(5)	180	178.7(1)
$C_\alpha-C_\beta-C_\beta$	108.4(7)	106(2)	106.7	107.0(8)
$C_\alpha-N_p-C_\alpha$	108.9(7)	106.2(13)	108.1	103.5(7)
$N_m-C_\alpha-N_p$	128.1(7)	127(2)	127.7	126.3(12)
$N_m-C_\alpha-N_p$	128.1(7)	127(2)	127.7	126.3(12)
$C_\alpha-N_m-C_\alpha$	122.6(5)	121.5(14)	123.2	120.8(19)
$N_p-C_\alpha-C_\beta$	108.8(6)	110.0(12)	109.3	110.0(14)
$C_\beta-C_\beta-S$	124.0(7)	123.1(13)		123.5(5)
$C_\alpha-C_\beta-S$	127.6(4)	129.4(14)		129.5(13)

[a] Averaged for Mg(pc), Zn(pc), Fe(pc), and Mn(pc) structures, except for $Ni-N_p$, which is taken from Ni(pc)I. See ref 25. [b] Reference 12.

interplanar separation between the nickel-coordinated nitrogen atoms of **11hB** is only slightly increased compared to **11hA** at 3.29 Å, but with the Ni···Ni separation markedly increased to 4.96 Å [cf. 3.41 Å for **A**], i.e., a lateral shift of 3.7 Å. The shortest intermolecular N···N contact within the **11hB** dimer is 3.34 Å between N(23) and its centrosymmetrically related counterpart.

The **11hA** dimer pairs form a stepped stack (Figure 3b) with the Pt-teeda units in one pair overlaying those of centrosymmetrically related pairs. The interpair Pt···Pt distances for **11hA** are 5.11 Å, precluding any significant interdimer interactions. Dimer pairs of **11hB** type molecules also from stepped stacks, though in this instance there is significant $\pi-\pi$ overlap between isoindole rings (*cis* to Pt) in adjacent, centrosymmetrically related dimer pairs (Figure 3c). The packing of **11hB** is quite similar to **11b**, but with a lesser degree of overlap of the fused benzo rings of adjacent dimers. In **11hB**, there is nearly 50% overlap between the six-membered ring components, with a ring-centroid···ring-centroid separation of 3.67 Å and a mean interplanar separation of 3.44 Å.

For **11h**, the type **A** and type **B** dimer pairs do not interact with each other, their respective planes being steeply inclined by *ca*. 51°. The intramolecular Ni···Pt distances are 7.12 and 7.10 Å for **A** and **B**, respectively. The shortest intermolecular Pt···Ni distance is 6.08 Å between the nickel atom of a type **A** molecule and the platinum atom of a type **B** moelcule. Again this is similar to the lack of interaction between the equivalent inclined stacks of **11b**.

Electronic Absorption Spectroscopy. The optical spectra of all porphyrazine derivatives exhibit two main bands, a Soret or B band ($\pi \rightarrow \pi^*$) between 330−375 nm and another beyond 650 nm, denoted the Q band ($\pi \rightarrow \pi^*$). The 4-fold symmetric macrocycles with four fused benzene rings (Ni(pc)) or four protected dithiolene moieties (Ni(obtp)) at the periphery have similar optical spectra, with single transitions for both the Q and B bands. In contrast, the optical spectra of unsymmetrical porphyrazines **6**−**10**, with three fused benzo rings and $n = 1$ protected dithiolene moiety, clearly show a splitting of the Q band (Figure 4). As discussed in the following paper (*J. Am.*

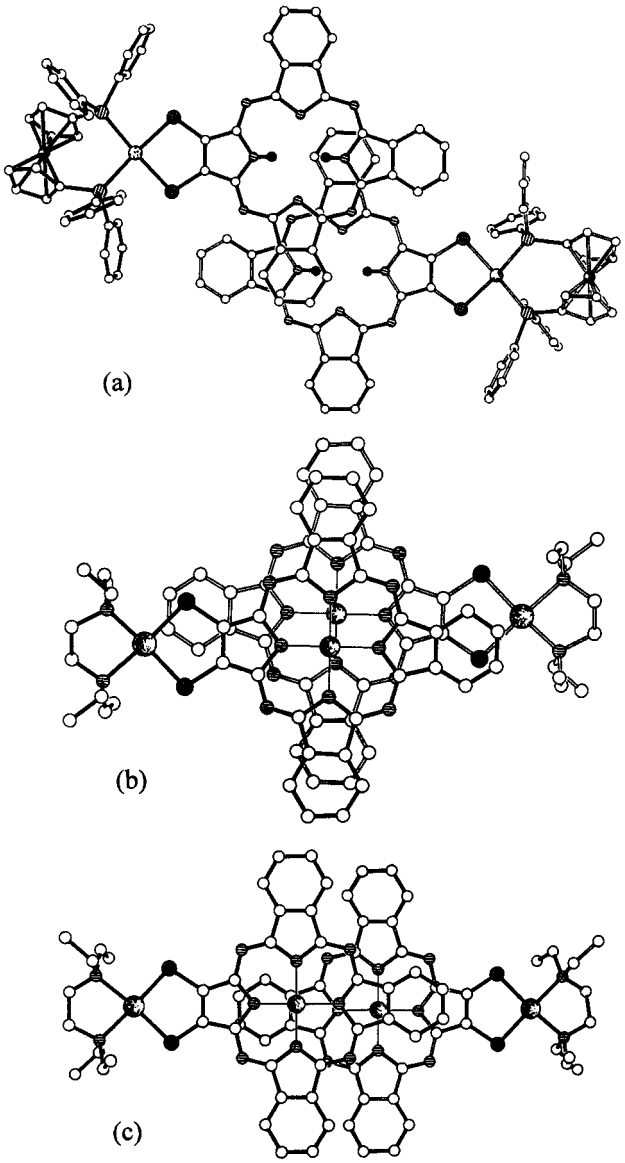

Figure 2. Parallel projection onto the mean plane of the four nickel-coordinated nitrogen atoms, showing the markedly different degree of overlap of pairs of centrosymmetrically-related molecules for (a)**11b**, (b)**11hA**, and (c)**11hB**.

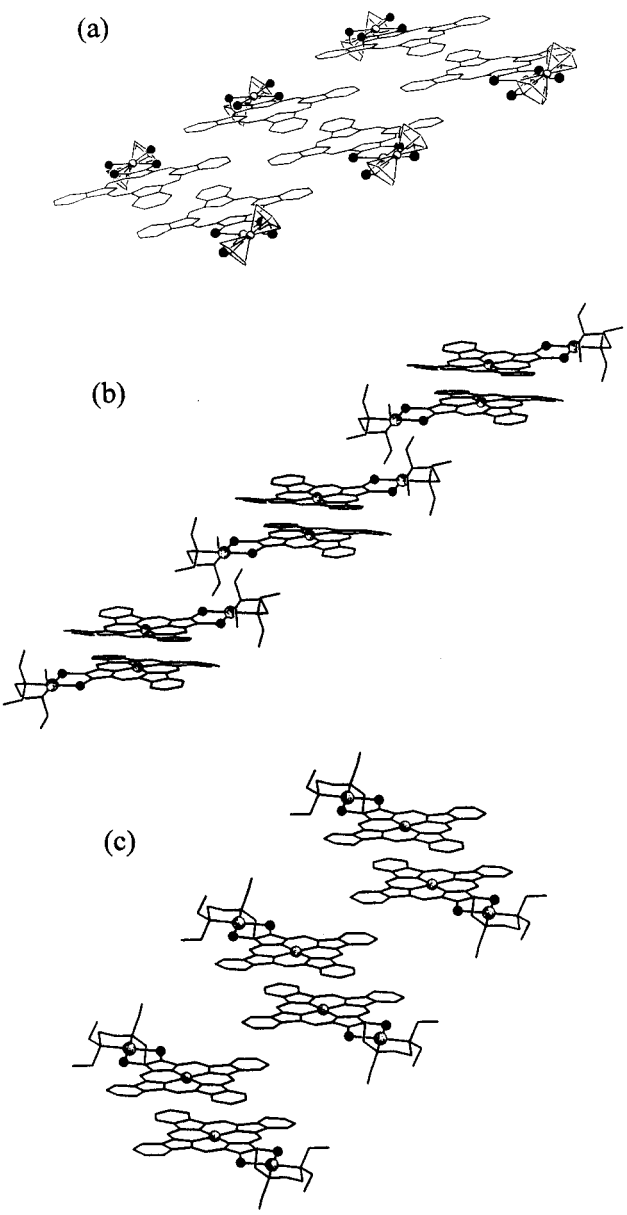

Figure 3. The stepped stack motif exhibited by the "dimer pairs" of molecules for (a)**11b**, (b)**11hA**, and (c)**11hB**. For clarity, the phenyl groups of the dppf ligand of **11b** have been omitted.

Chem. Soc. **1996**, *118*, 10487),[13] these differences can be rationalized through Gouterman's highly simplified four orbital model[29] for the optical spectra of porphyrins and porphyrazines.

Surprisingly, the peripherally metalated *solitaire*-porphyrazines do not show a splitting of the Q-band: their optical spectra look quite like those of an M(pc) (Figure 4). This effect might reflect a modest extension of the porphyrazine π-system into the five-membered chelate ring mediated by the dithiolate moiety. Alternatively, a metal ion bound to the sulfurs might significantly change their ability to donate electrons to the porphyrazine ring, accidentally undoing the change in the relative energies of the frontier orbitals.

Electron Paramagnetic Resonance. Whereas the optical spectra provide evidence as to perturbations of the porphyrazine π-system by peripheral substitutions, EPR studies of the unpaired σ-electron on the Cu^{2+} of a Cu(porphyrazine) provide evidence as to perturbations of the σ-system. The EPR spectrum at 77 K of a powder sample of 1% Cu *solitaire*-porphyrazine **11d** magnetically diluted in its diamagnetic host **11b** shows axial symmetry as is typical for monomeric square-planar Cu(II) complexes[21,30,31] with resolved ^{63}Cu and ^{14}N hyperfine. The spin Hamiltonian parameters are listed in Table 3. Interestingly, the parameters for **11d** fall between those of Cu(omtp)[23] and Cu(pc),[31] showing there are no more than small effects of functionalization at the macrocyclic periphery on the electronic structure of the central Cu(II) ion. The Mn(III) porphyrazines, **10** and **11g**, are EPR silent at 77 K consistent with an even-spin d^4 system.[32]

Electrochemistry of *solitaire*-Porphyrazines. Typical phthalocyanines and porphyrins undergo two ring oxidations and up to four successive ring reductions.[33,34] For phthalocya-

(28) Lever, A. B. P. *Adv. Inorg. Chem. Radiochem.* **1965**, *7*, 28.
(29) Gouterman, M. In *The Porphyrins*; Dolphin, D., Ed.; Academic Press: New York, 1978; Vol. III, pp 1−165.
(30) Harrison, S. E.; Assour, J. M. *J. Chem. Phys.* **1964**, *40*, 365.
(31) Brown, T. G.; Peterson, J. L.; Lozos, G. P.; Anderson, J. R.; Hoffman, B. M. *Inorg. Chem.* **1977**, *16*, 1563.
(32) Lever, A. B. P. *J. Chem. Soc.* **1965**, 1821.
(33) Bottomley, L. A.; Chiou, W. J. H. *J. Electroanal. Chem.* **1986**, *198*, 331−346.
(34) (a) Clark, D. W.; Hush, N. S. *J. Am. Chem. Soc.* **1965**, *87*, 4238. (b) Clark, D. W.; Yandle, J. R. *Inorg. Chem.* **1972**, *11*, 1738.

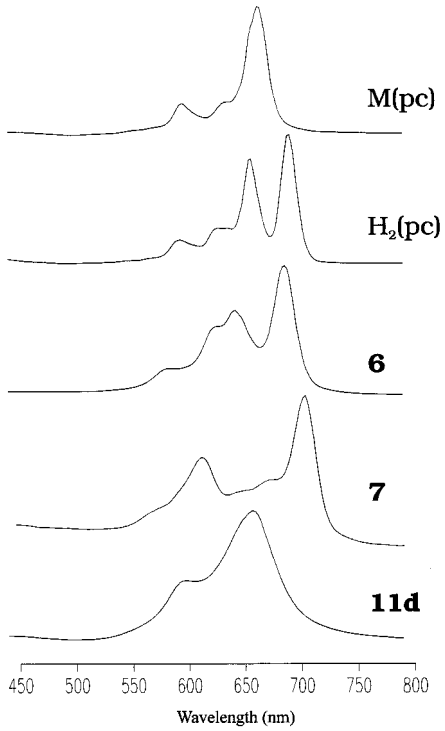

Figure 4. Comparison of the Q band region for both metalated and metal-free phthalocyanine with compounds **6**, **7**, and **11d** (20 μM in CH_2Cl_2).

Table 3. EPR Parameters for *solitaire*-Porphyrazine **11d** and Related Cu(II) Macrocycles[a]

complex	$g_{\|\|}$	$A_{\|\|}^{Cu}$	A^N	B^N
Cu(pc)[b]	2.18	604	53.4	40.7
11d;9[c]	2.16	635	55.9	41.6
Cu(omtp)[d]	2.14	644	57.4	43.3

[a] Hyperfine coupling constants are expressed in units of megahertz. [b] Reference 32. [c] Values for the two compounds are indistinguishable. [d] Reference 23.

nines specifically, the reductions are usually reversible, but the oxidations are not. As representatives of the compounds prepared here, the electrochemistry of *solitaire*-porphyrazine **11b** and the precursor **7** was examined. Within the accessible potential range of the CH_2Cl_2/tetrabutylammonium hexafluorophosphate solvent/electrolyte system, both macrocycles exhibit two reversible one-electron reductions, which, likewise, are attributed to reductions of the porphyrazine ring π-system. As seen in Table 4, the potentials for the ring reductions of both **7** and the *solitaire*-porphyrazine **11b** occur at ~ -1.20 and ~ -1.60 V (vs Fc^+/Fc), essentially the same as for H_2(pc) but significantly higher than for H_2(obtp) (-0.85 and -1.19 V). Within the limit of $+150$ V as determined by the solvent (CH_2Cl_2), no ring oxidation were observed for either **7** or **11b**.

For *solitaire*-porphyrazines with the coordinated [1,1′-(diphenylphosphino)ferrocene]palladium(II) cap, **11b**−**d**, the cyclic voltammogram showed a reversible one electron oxidation

Table 4. Comparison of Half-Wave Potentials[a] of the Ring Reductions, RR's, for **7**, **11b**, H_2(obtp), and H_2(pc)

macrocycle	$E_{1/2}(RR^1)$	$E_{1/2}(RR^2)$
7	-1.23	-1.59
11b	-1.27	-1.51
H_2(pc)[b]	-1.20	-1.54
H_2(obtp)	-0.85	-1.19

[a] Half-wave potentials are reported vs (Fc^+/Fc) couple. The electrochemistry for **7**, **11b**, and **H**$_2$(obtp) were performed in CH_2Cl_2 with 0.1 M $TBAPF_6$ as the electrolyte using a Pt working electrode and a Ag/AgCl reference electrode. [b] Reference 35.

associated with the ferrocene portion of the diphosphine ligand ($+0.18$ V vs Fc^+/Fc). There also appears to be an irreversible wave, $+0.63$ mV vs (Fc^+/Fc), most likely associated with a Pd(III/II) oxidation. Unlike the metal bis(dithiolene) systems that undergo a reversible M(III/II) oxidation,[35] this [S_2MP_2] ligand environment is unable to stabilize the oxidized metal center. Such an irreversible wave is seen for all the other (P−P)M(II)-capped *solitaire*-porphyrazines, **11a**−**g**. *solitaire*-Porphyrazine **11h**, on the other hand, appears to show a reversible oxidation at $+0.43$ mV (vs Fc^+/Fc) that is associated with the oxidation of the peripheral [S_2PtN_2] unit. The amine nitrogens of the teeda ligand are better σ-donors than the phosphorus ligands and apparently they stabilize the oxidized metal center better. The details of this oxidation process are currently under investigation.

Acknowledgment. This work was supported by the National Science Foundation (CHE-9408561).

Supporting Information Available: For complex **11b**: Figure showing the numbering scheme, displacements from the least-squares plane, and unit cell packing diagrams and tables of crystal data and structure refinement, atomic coordinates and equivalent isotropic displacement parameters, bond lengths and angles, anisotropic displacement parameters, and hydrogen coordinates and isotropic displacement parameters. For complex **11h**: Figure showing the numbering scheme, side view of **11hA** showing the pronounced dishing of the porphyrazine (Figure S1), the side view of **11hB** showing the noticeably more planar conformation of the porphyrazine core (Figure S2), and tables of crystal data and structure refinement, atomic coordinates and equivalent isotropic displacement parameters, bond lengths and angles, anisotropic displacement parameters, and hydrogen coordinates and isotropic displacement parameters. A table of elemental analyses for the BCB-protected precursors, **6**−**10**, and *solitaire*-porphyrazines, **11a**−**h**, is included along with a table of their electronic absorption maxima and molar extinction coefficients (31 pages). See any current masthead page for ordering and Internet access information.

JA9619115

(35) (a) Davison, A.; Edelstein, N.; Holm, R. H.; Maki, A. H. *Inorg. Chem.* **1963**, *2*, 1227−1232. (b) Billig, E.; Williams, R.; Bernal, I.; Waters, J. H.; Gray, H. B. *Inorg. Chem.* **1964**, *3*, 663−666. (c) Vance, C. T.; Bereman, R. D. *Inorg. Chim. Acta* **1988**, *149*, 229−234.